

Comparative study of Au and Ni/Au gated AlGaN/GaN high electron mobility transistors

Cite as: AIP Advances 9, 125231 (2019); <https://doi.org/10.1063/1.5116356>

Submitted: 24 June 2019 • Accepted: 03 December 2019 • Published Online: 23 December 2019

 Ajay Kumar Visvkarma, Chandan Sharma, Robert Laishram, et al.



View Online



Export Citation



CrossMark

ARTICLES YOU MAY BE INTERESTED IN

[Two-dimensional electron gases induced by spontaneous and piezoelectric polarization charges in N- and Ga-face AlGaN/GaN heterostructures](#)

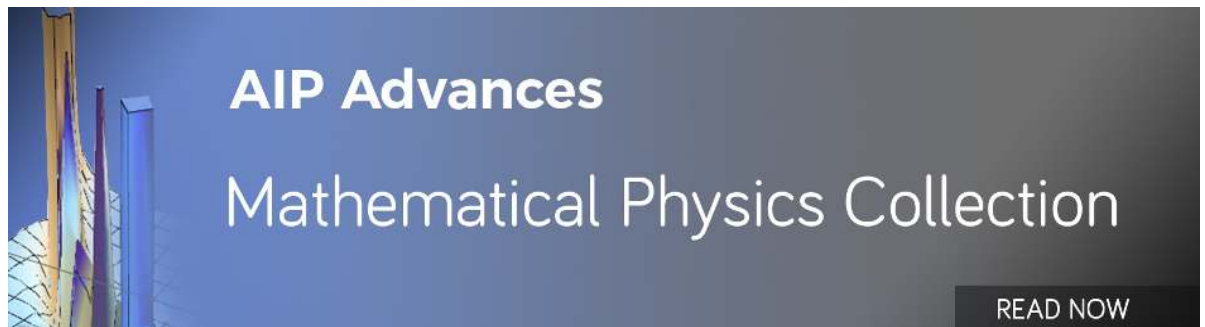
Journal of Applied Physics **85**, 3222 (1999); <https://doi.org/10.1063/1.369664>

[Two dimensional electron gases induced by spontaneous and piezoelectric polarization in undoped and doped AlGaN/GaN heterostructures](#)

Journal of Applied Physics **87**, 334 (2000); <https://doi.org/10.1063/1.371866>

[Polarization effects, surface states, and the source of electrons in AlGaN/GaN heterostructure field effect transistors](#)

Applied Physics Letters **77**, 250 (2000); <https://doi.org/10.1063/1.126940>



Comparative study of Au and Ni/Au gated AlGaIn/GaN high electron mobility transistors

Cite as: AIP Advances 9, 125231 (2019); doi: 10.1063/1.5116356

Submitted: 24 June 2019 • Accepted: 3 December 2019 •

Published Online: 23 December 2019



Ajay Kumar Visvkarma,^{1,2}  Chandan Sharma,³ Robert Laishram,² Sonalee Kapoor,² D. S. Rawal,^{2,a)} 
Seema Vinayak,² and Manoj Saxena⁴

AFFILIATIONS

¹Semiconductor Device Research Laboratory, Department of Electronic Science, University of Delhi, South Campus, New Delhi 110021, India

²MMIC Fabrication Division, Solid State Physics Laboratory, Lucknow Road, Delhi 110054, India

³Department of Physics, Indian Institute of Technology Delhi, Hauz Khas, New Delhi 110016, India

⁴Department of Electronics, Deen Dayal Upadhyaya College, University of Delhi, New Delhi 110078, India

^{a)} Author to whom correspondence should be addressed: dsrawal15@gmail.com

ABSTRACT

This paper presents the electrical comparison of Au and Ni/Au gated HEMT devices and diodes. Au Schottky diodes on an AlGaIn/GaN heterostructure exhibit better electrical performance in comparison to conventional Ni/Au diodes with an improved Schottky barrier height (SBH) and lower reverse leakage current. The SBH extracted from I-V for Au and Ni/Au is 1.29 eV and 0.74 eV, respectively. Au Schottky contacts on GaN have a better ideality factor of 1.55 than Ni, which is 1.61. Capacitance-voltage measurement revealed a positive shift in threshold voltage in the case of Au diodes with a reduced capacitance value with respect to Ni/Au diodes. This decrease in threshold and capacitance indicates a decrease in the 2DEG carrier concentration. The decrease in the 2DEG carrier concentration is consistent with three terminal device measurements. Despite a small decrease in drain current (8%), the Au gated HEMT devices have shown an improved subthreshold slope (13%) and nearly 4 order improvement in the I_{ON}/I_{OFF} ratio than Ni/Au gated HEMTs. Pulse IV characterization has indicated that gate lag and drain lag have no major changes with respect to gate metal, whereas current collapse increases for high work function metals.

© 2019 Author(s). All article content, except where otherwise noted, is licensed under a Creative Commons Attribution (CC BY) license (<http://creativecommons.org/licenses/by/4.0/>). <https://doi.org/10.1063/1.5116356>

INTRODUCTION

Wide bandgap III-V semiconductor materials like gallium nitride (GaN) and its doped family members (AlGaIn/InGaIn) possess incredible material properties like high and direct bandgap, high thermal conductivity, and high breakdown electric field in comparison to conventional semiconductors like silicon and gallium arsenide (GaAs). These properties make III-V materials suitable for power electronics, photonic applications, sensing, and space applications.¹⁻⁴ Also, the existence of spontaneous and piezoelectric polarizations in the AlGaIn/GaN system is responsible for the formation of a two dimensional electron gas (2DEG) channel with high carrier density and high mobility at the hetero-interface without any doping.^{5,6} AlGaIn/GaN hetero-structure based HEMT devices have also made a tremendous progress in the field of RF and space

applications. The performance of GaN-HEMT devices is a strong function of both ohmic and Schottky metal contacts. Since the gate contact is Schottky in nature, it has total control over the current conduction in a channel. A majority of work in this area is being carried out to further improve their characteristics to achieve better device performance using different gate metals and gate dielectric and in the application of field plate structures.⁷⁻¹¹ Even with plenty of advantages offered by GaN-HEMTs, gate reverse leakage in GaN-HEMTs has been the area of focus for further improvement. In order to improve the gate characteristics of GaN-HEMTs, the Schottky contact on the GaN and AlGaIn/GaN hetero-structure has been studied with numerous metals including Al, Ti, Ni, Au, and Pt and other refractory metals.¹²⁻¹⁶ The improvement in Schottky diode characteristics is well reported with Au Schottky contacts on GaN. To the best of our knowledge, not much literature is available

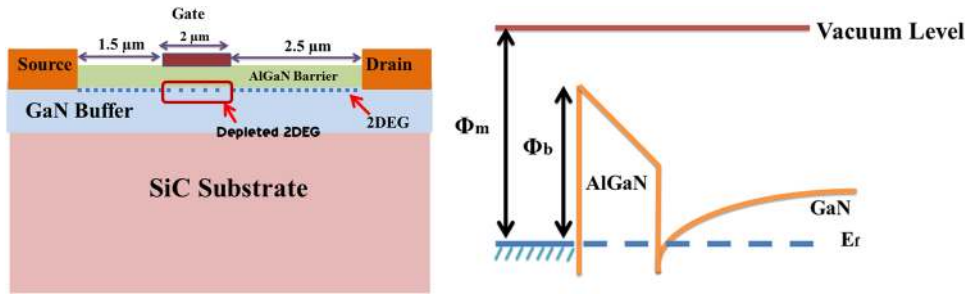


FIG. 1. Schematic diagram of the fabricated AlGaIn/GaN HEMT device and conduction band diagrams for the Schottky gate on AlGaIn/GaN.

for Au gated AlGaIn/GaN HEMTs. In this work, we are presenting a comparative study of Au and Ni/Au based diodes and HEMTs on the AlGaIn/GaN hetero-structure. Au based diodes are found to be superior to Ni/Au based diodes, which is in concurrence with the available literature. The HEMT devices having Au and Ni/Au as gate contact metals have also been compared, which reveals improvements in the subthreshold slope and I_{ON}/I_{OFF} ratio with a small reduction in drain current.

EXPERIMENTAL DETAILS

The HEMT epitaxial layer structure used in this study has been grown in-house via the metal organic chemical vapor deposition (MOCVD) technique in an Aixtron reactor. The layer structure consists of an $Al_{0.23}Ga_{0.77}N$ barrier layer of 24 nm over a GaN buffer layer of 2.5 μm on a SiC substrate. Contactless hall measurement showed a 2DEG concentration of $1.1 \times 10^{13} cm^{-2}$ with a 2DEG mobility of 1900 cm^2/Vs . Device fabrication involves source/drain ohmic contact formation, mesa etching, and gate writing. Metalization has been performed via the lift off technique. The ohmic metal stack consisting of Ti/Al/Ni/Au has been deposited using the electron beam evaporation system followed by RTA at 820 $^{\circ}C$ for 90 s in vacuum leading to the formation of an ohmic contact on the AlGaIn/GaN epistucture. Mesa etching is carried out using the Oxford reactive ion etching (RIE) system involving BCl_3/Cl_2 based chemistry. After mesa etching, gate metals were deposited using an electron beam evaporation system. The thickness of gate metals [Ni/Au (400/1100 \AA) and Au (1500 \AA)] is kept the same. Dimensions of the fabricated devices are shown in Fig. 1. Circular transmission line method (CTLM) measurements, two terminal diode measurements, and three terminal device measurements were recorded at room temperature with the same environment conditions using the semiconductor parametric analyzer B1500. The contact resistance and FOM have been extracted through CTLM measurements and are 1.4 Ω and 0.44 Ω -mm, respectively.

EXPERIMENTAL RESULTS

The fabricated device was electrically tested on the semiconductor parametric analyzer (SPA) B1500 at room temperature.

Two terminal diode measurements

I-V characteristics of the Schottky diode formed between the gate metal (Au and Ni/Au) and AlGaIn surface are shown in Fig. 2.

The Schottky barrier height (SBH) and ideality factor for respective gate metals have been calculated using the following standard diode equations and are tabulated in Table I:

$$J = J_s \left[\exp\left(\frac{qV}{\eta kT}\right) - 1 \right], \quad (1)$$

$$J_s = A^* T^2 \exp(-q\Phi_b/kT), \quad (2)$$

where J_s is the reverse saturation current density, Φ_b is the SBH, A^* is the Richardson constant, η is the ideality factor, q is the charge of an electron, k is Boltzmann's constant, and T is the temperature of measurement.¹⁷

Improvement in the SBH and ideality factor is achieved with the Au Schottky diode, which is well supported by the literature;¹³ this improvement in the SBH is likely due to the combined effect of improvement in the inhomogeneities at the metal-semiconductor interface and the higher work function of Au in comparison to Ni.¹³ A rapid two order increase in the reverse leakage current between -2 V and -5 V is observed with the Ni/Au Schottky diode compared with the Au Schottky diode. This rapid rise is due to the high carrier

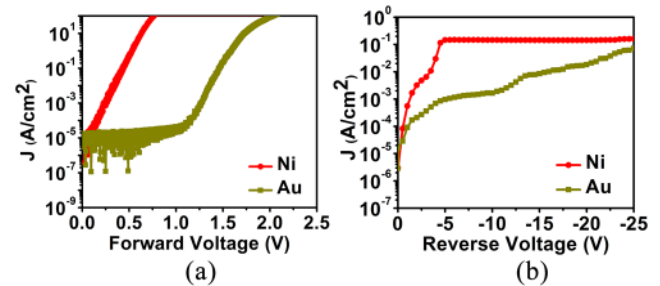


FIG. 2. (a) Diode forward I-V curves for Au and Ni/Au Schottky diodes on AlGaIn/GaN HEMT and (b) diode reverse I-V curves for Au and Ni/Au Schottky diodes on AlGaIn/GaN HEMT.

TABLE I. Extracted parameters from the two terminal diode measurements, I-V and C-V.

Metal	Φ_m (eV)	SBH (eV)	η	V_{TH} (V)
Au	5.3	1.29	1.55	-4.32
Ni/Au	5.1	0.74	1.61	-4.71

injection rate from Ni to AlGaIn since the barrier height achieved with nickel is comparatively smaller than that achieved with gold. At high reverse bias, the rate of increase in current has reduced and is almost saturated in the case of nickel. This is dedicated to the trapping of carriers in the AlGaIn layer at high reverse bias.^{10,18,19}

Capacitance voltage (CV) measurement is carried out at 1 MHz for both diodes to get a better insight into the diode and the HEMT device. The gold Schottky diode is observed to have a more positive threshold voltage ($\Delta V = 0.39$ V) with a comparable capacitance value, as shown in Fig. 3(a).

Changes in 2DEG carrier concentrations (n_{2DEG}) below the gate metal after device fabrication were also evaluated using the following equation, and, as evident from the graph, Au has a slight reduction in the 2DEG carrier concentration. The decrease in the 2DEG carrier concentration points to the condition of more depletion of the 2DEG channel under Au contact than Ni since Au has a higher work function than Ni,

$$n_{2DEG} = \int N(w)dw = \frac{2}{q\epsilon A^2 d(1/C^2)/dV}, \quad (3)$$

where $N(w)$ is the carrier contraction of 2DEG in cm^{-3} , w is the depletion width, C is the measured capacitance value, A is the area of the gate metal ($2 \times 200 \mu m^2$), ϵ is the permittivity of AlGaIn, and q is the elementary charge.²⁰ The comparative decrease in 2DEG concentration is $0.31 \times 10^{13} cm^{-2}$; this reduction is well reflected in the device I-V measurements.

Figure 3(b) shows the conductance-voltage (GV) plot of the same device measured at 1 MHz frequency. The Au gated device has a lower conductance in the off state than the Ni/Au gated device. This reduction in conductance implies that the Au gate shows an improvement in the off state leakage current. It can be related to the difference in the number of available defect sites at the metal-semiconductor interface which are responsible for trapping and de-trapping of carriers. Au is expected to have a fewer number of defect sites at the interface than Ni/Au and hence show improvement in the leakage characteristics.

In conclusion, the Au Schottky diodes on AlGaIn/GaN are found to exhibit better performance. The positive shift in the threshold voltage (V_{TH}) in CV is of great importance; as HEMT devices are depletion mode devices, the positive shift in threshold will bring the

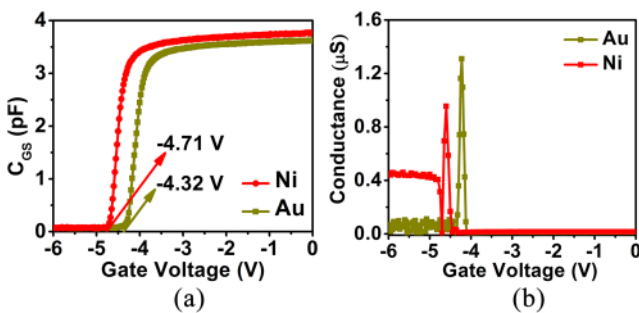


FIG. 3. (a) CV of Au and Ni/Au Schottky diodes measured at 1 MHz; the Au Schottky diode has a lower threshold voltage. (b) Conductance-voltage characteristic curve measured between the gate and source at 1 MHz.

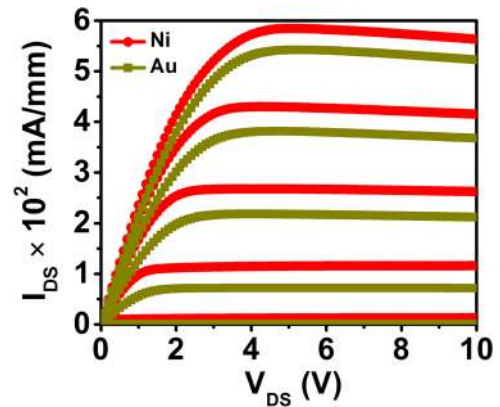


FIG. 4. Output characteristics of Au and Ni/Au gated AlGaIn/GaN HEMT; V_G is varied from -6 V to 0 V.

device toward the enhancement mode side. Hence, it can be turned off at a lower voltage. Moreover, we believe that the effective work function for Ni is lower than 5.1 eV as the observed SBH is quite lower than that previously reported by the literature.^{12,13,21}

Three terminal device measurements

After characterizing the diode electrically, the device characteristics were recorded using an SPA B1500A. The device output characteristic and transfer characteristics of the Au and Ni/Au gated device are compared, as shown in Figs. 4 and 5, respectively.

The drain current in the Au gated HEMT device is slightly lower ($\approx 8\%$) than the Ni/Au gated device, which is a clear indication for the slight decrease in the 2DEG carrier concentration below the gate region. As explained earlier, this decrease in the 2DEG carrier concentration is due to higher depletion of 2DEG by Au than Ni, which is a combined effect of the comparatively high work function of Au and improvement in the interface inhomogeneities revealed by the two terminal measurements. The transfer characteristic (Fig. 5) shows that the Au gated HEMT device shows a strong improvement in the I_{ON}/I_{OFF} ratio which is nearly of 4 orders. Also,

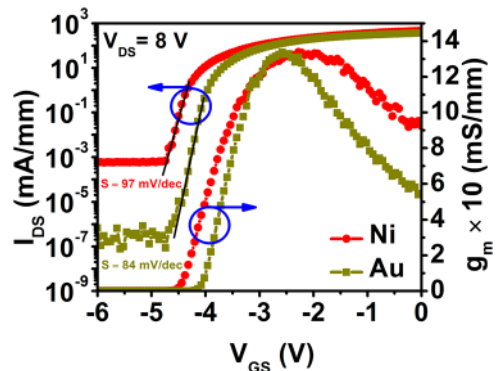


FIG. 5. Transfer characteristics of Au and Ni/Au gated AlGaIn/GaN HEMT; V_{DS} is fixed at 8 V.

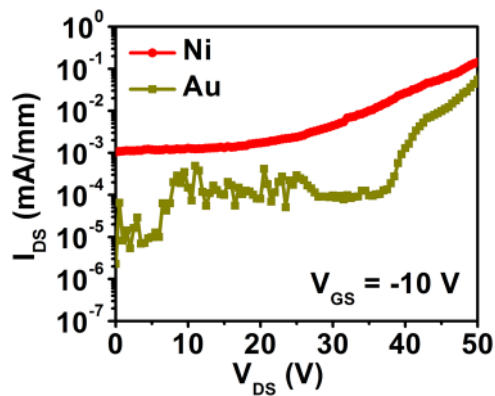


FIG. 6. Three terminal reverse breakdown measured at the gate biased at -10 V.

an improvement in the subthreshold slope (S) is achieved with Au gated HEMTs, which makes them a suitable selection for switching applications.

The positive shift in the threshold voltage (V_{TH}) of transfer characteristics matches well with the shift observed in CV of the diodes. This shift is pointing to the reduction in n_{2DEG} . The positive shift makes Au gated HEMTs more energy efficient as a lower negative voltage is required to turn off the device. Figure 6 shows the three terminal reverse breakdowns which were measured for these devices keeping the gate biased at -10 V. Both devices nearly experienced the same breakdown with a little lower leakage in the Au gated HEMT device until -40 V.

Pulse measurements were carried out using the GaAs Code pulse I-V system, which is capable of generating pulses with a minimum width of 200 ns. The gate and drain of the both devices are biased with different quiescent points, as shown in Fig. 7, to observe the effect of the gate metal on drain lag, gate lag, and overall current collapse. Figure 7 shows the comparison of Au and Ni/Au gated HEMTs (those with only $V_{GS} = 0$ V are shown). The circles (solid and empty) are for Ni/Au HEMT, and the squares (solid and empty) are for Au gated HEMT.

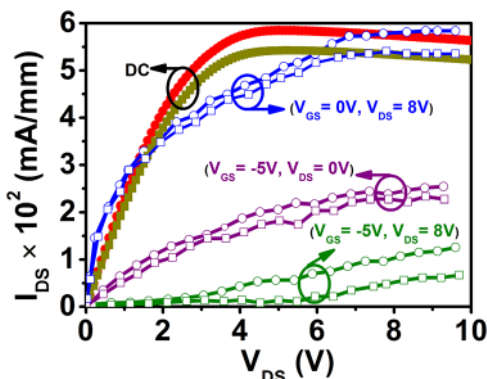


FIG. 7. Comparison of the DC (solid symbol) vs pulse (empty symbols) measurement carried out at different bias points. Circles (solid and empty) and squares (solid and empty) are marked for Ni/Au and Au gated HEMTs, respectively (only $V_{GS} = 0$ V are shown for easy understanding that is at a zero bias condition).

are marked for Au gated HEMT. The drain lag and gate lag is almost similar in both the devices, whereas the current collapse is slightly higher in the case of the Au gate HEMT device. This may be probably due to the contribution of an additional gate field developed under the gate region in the case of Au in comparison to Ni as the Au Schottky contact is seen to undergo an enhancement in the depletion region.

CONCLUSION

Au and Ni/Au gated HEMT devices were fabricated on an AlGaIn/GaN HEMT epistructure. Au exhibits better Schottky performance in terms of the Schottky barrier height and reverse leakage with an improved ideality factor. The CV reveals better gate characteristics of the Au Schottky contact in comparison to Ni/Au Schottky contacts with a lower threshold value of $\Delta V = 0.39$ V and with almost the same gate capacitance. This shift in threshold with Au gated GaN HEMT devices is positive in nature, shifting them toward enhancement mode devices. Three terminal I-V measurements were also performed for Au and Ni/Au gated HEMTs that reveal nearly a four order improvement in the I_{ON}/I_{OFF} ratio along with a 13% improvement in the subthreshold slope for Au gated HEMTs with a little reduction in the drain current. The positive shift in CV and the decrease in drain current confirm the reduction in the 2DEG channel carrier concentration under the gate region, which is metal and interface dependent. The pulse measurements were carried out to understand the effect of drain lag, gate lag, and current collapse with respect to the gate metal. The drain lag and gate lag is observed to be of the same order for both gate metals, indicating that gate metals (Ni and Au) have no major effect on these parameters, whereas the degree of current collapse is higher for the high work function gate metal, indicating enhanced trapping in Au gate HEMTs.

ACKNOWLEDGMENTS

The authors are thankful to the Solid State Physics Laboratory (SSPL) for providing the necessary opportunity to carry out this work and to the whole SSPL GaN-MMIC group for their valuable support.

REFERENCES

- U. K. Mishra, L. Shen, T. E. Kazior, and Y.-F. Wu, "GaN-based RF power devices and amplifiers," *Proc. IEEE* **96**(2), 287–305 (2008).
- H. Okumura, "Present status and future prospect of wide gap semiconductor high-power devices," *Jpn. J. Appl. Phys., Part 1* **45**(10A), 7565–7586 (2006).
- N. M. Triet, Le T. Duy, B.-U. Hwang, A. Hanif, S. Siddiqui, K. H. Park, C.-Y. Cho, and N.-E. Lee, "High-performance Schottky diode gas sensor based on heterojunction of three-dimensional nano-hybrids of reduced graphene oxide–vertical ZnO nanorods on AlGaIn/GaN layer," *ACS Appl. Mater. Interfaces* **9**(36), 30722–30732 (2017).
- R. S. Pengelly, S. M. Wood, J. W. Milligan, S. T. Sheppard, and W. L. Pribble, "A review of GaN on SiC high electron mobility power transistors and MMICs," *IEEE Trans. Microwave Theory Tech.* **60**(6), 1764–1783 (2012).
- O. Ambacher, J. Smart, J. R. Shealy, N. G. Weimann, K. Chu, M. Murphy, W. J. Schaff, L. F. Eastman, R. Dimitrov, L. Wittmer, M. Stutzmann, W. Rieger, and J. Hilsenbeck, "Two-dimensional electron gases induced by spontaneous and piezoelectric polarization charges in N- and Ga-face AlGaIn/GaN heterostructures," *J. Appl. Phys.* **85**(6), 3222–3233 (1999).

- ⁶J. P. Ibbetson, P. T. Fini, K. D. Ness, S. P. DenBaars, J. S. Speck, and U. K. Mishra, "Polarization effects, surface states, and the source of electrons in AlGaIn/GaN heterostructure field effect transistor," *Appl. Phys. Lett.* **77**(2), 250–252 (2000).
- ⁷A. Suzuki, K. Akira, J. T. Asubar, H. Tokuda, and M. Kuzuhara, "Improved current collapse in AlGaIn/GaN HEMTs with 3-dimensional field effect structure," in *Technical Digest, IEEE International Meeting on Future of Electron Devices, Kansai* (IEEE, 2015), p. 36.
- ⁸W. Long, H. Ou, J.-M. Kuo, and K. K. Chin, "Dual-material gate (DMG) field effect transistor," *IEEE Trans. Electron Devices* **46**(5), 865–870 (1999).
- ⁹A. K. Visvkarma, R. Laishram, S. Kapoor, D. S. Rawal, S. Vinayak, and M. Saxena, *Semicond. Sci. Technol.* **34**, 105013 (2019).
- ¹⁰R. T. Green, I. J. Luxmoore, K. B. Lee, P. A. Houston, F. Ranalli, T. Wang, P. J. Parbrook, M. J. Uren, D. J. Wallis, and T. Martin, "Characterization of gate recessed GaIn/AlGaIn/GaN high electron mobility transistors fabricated using a SiCl₄/SF₆ dry etch recipe," *J. Appl. Phys.* **108**, 013711 (2010).
- ¹¹Y. Kang, H.-k. Sung, and H. Kim, "Investigation of kink effect in normally-off AlGaIn/GaN recessed-gate MOS-heterostructure FETs," *J. Vac. Sci. Technol., B* **34**, 052202 (2016).
- ¹²J. Zhao, Z. Lin, Q. Chen, M. Yang, P. Cui, Y. Lv, and Z. Feng, "A study of the impact of gate metals on the performance of AlGaIn/AlN/GaN heterostructure field-effect transistors," *Appl. Phys. Lett.* **107**, 113502 (2015).
- ¹³J.-H. Shin, J. Park, S. Y. Jang, T. Jang, and K. S. Kim, "Metal induced inhomogeneous Schottky barrier height in AlGaIn/GaN Schottky diode," *Appl. Phys. Lett.* **102**, 243505 (2013).
- ¹⁴T. Kawanago, K. Kakushima, Y. Kataoka, A. Nishiyama, N. Sugii, H. Wakabayashi, K. Tsutsui, K. Natori, and H. Iwai, "Advantage of TiN Schottky gate over conventional Ni for improved electrical characteristics in AlGaIn/GaN HEMT," in *ESSDERC* (IEEE, 2013), pp. 107–110.
- ¹⁵M. Lee, T. K. Oanh Vu, K. Su Lee, E. K. Kim, and S. Park, "Electronic transport mechanism for Schottky diodes formed by Au/HVPE a-plane GaN templates grown via in situ GaN nanodot formation," *Nanomaterials* **8**(6), 397 (2018).
- ¹⁶D. Qiao, L. S. Tu, and S. S. Lau, "Dependence of Ni/AlGaIn Schottky barrier height on Al mole fraction," *J. Appl. Phys.* **87**(2), 801–804 (2000).
- ¹⁷S. M. Sze, *Physics of Semiconductor Devices* (Wiley, New York, 2007).
- ¹⁸E. J. Miller, X. Z. Dang, and E. T. Yu, "Gate leakage current mechanisms in AlGaIn/GaN heterostructure field-effect transistors," *J. Appl. Phys.* **88**(10), 5951–5958 (2000).
- ¹⁹W. S. Tan, M. J. Uren, P. A. Houston, R. T. Green, R. S. Balmer, and T. Martin, "Surface leakage currents in SiN_x passivated AlGaIn/GaN HFETs," *IEEE Electron Device Lett.* **27**(1), 161–163 (2006).
- ²⁰D. K. Schroder, *Semiconductor Material and Device Characterization*, 3rd ed. (Wiley, 2006).
- ²¹M. Garg, T. R. Naik, R. Pathak, V. R. Rao, C.-H. Liao, K.-H. Li, H. Sun, X. Li, and R. Singh, "Effect of surface passivation process for AlGaIn/GaN HEMT heterostructures using phenol functionalized-porphyrin based organic molecules," *J. Appl. Phys.* **124**, 195702 (2018).